DMD Fast Forward. Published on December 9, 2010 as doi:10.1124/dmd.110.036376
This article has not been copyedited and formatted. The final version may differ from this version.

SIMPLE, DIRECT AND INFORMATIVE METHOD FOR THE ASSESSMENT OF CYP2C19 ENZYME INACTIVATION KINETICS

Kaisa A. Salminen, Jukka Leppänen, Jarkko I. Venäläinen, Markku Pasanen, Seppo Auriola, Risto O. Juvonen, and Hannu Raunio

School of Pharmacy, Faculty of Health Sciences, University of Eastern Finland, Kuopio, Finland (K.A.S., J.L., M.P., S.A., R.O.J., H.R.); and Orion Corporation, ORION PHARMA, Research and Development, Turku, Finland (J.I.V.)

Running title: DBF for kinetic assay and analysis of CYP2C19 inhibition

Address correspondence to:

Kaisa A. Salminen, M.Sc. (in Pharmacy)

School of Pharmacy

Faculty of Health Sciences

University of Eastern Finland

P.O. Box 1627

70211 Kuopio, Finland

Phone: +358 40 355 3774

Fax: +358 17 162424

E-mail: kaisa.salminen@uef.fi

Text Pages: 29

Tables: 4

Figures: 7

References: 33

Words in Abstract: 249

Words in Introduction: 667

Words in Discussion: 968

Abbreviations: DBF, dibenzylfluorescein; MBI, mechanism-based inactivation; CYP, cytochrome P450.

Abstract

Many clinically relevant drug interactions involving CYP inhibition are mediated by mechanism-based inactivation (MBI). Time-dependent inhibition is one of the major features distinguishing between reversible inhibition and MBI. It thus provides a useful screening approach for early drug interaction risk assessment. Accordingly, we developed an easy and informative fluorometric method for the assessment of CYP2C19 enzyme inactivation kinetics. Dibenzylfluorescein (DBF) is widely used as pro-fluorescent probe substrate for CYP activity and inhibition assays, but its use has been considered to be limited to traditional end-point assays. We monitored CYP2C19 catalyzed metabolism of DBF using synthesized fluorescein benzyl ester and fluorescein benzyl ether along with commercially available fluorescein as intermediate standards. Furthermore, we demonstrated the use of DBF in a kinetic assay as a progress curve analysis for straightforward determination if a compound is a time-dependent inactivator of CYP2C19. The recombinant human CYP2C19 inactivation kinetics of isoniazid, ticlopidine, and tranylcypromine were evaluated and their key kinetic parameters were measured from the same experiment. The known mechanism-based inactivators, isoniazid and ticlopidine, exhibited clear time-dependent inactivation with K_I and k_{inact} values of 250.5 ± 34 μM and 0.137 ± 0.006 min^{-1}; and 1.96 ± 0.5 μM and 0.135 ± 0.009 min^{-1}, respectively. Tranylcypromine did not display any time-dependent inhibition which is consistent with its reported mechanism of competitive inhibition. In summary, DBF is suitable for use in the progress curve analysis approach and can be used as an initial screen to identify compounds that require more detailed investigations in drug interaction optimization.

Introduction

The human cytochrome P450 (CYP) enzymes play an important role in the metabolism of drugs and numerous other xenobiotics. Inhibition of CYP enzymes is a common mechanism which can lead to drug interactions. These can evoke severe adverse effects, they have resulted in early termination of drug development, refusal to obtain approval, prescribing restrictions, and even withdrawal of drugs from the market (Wienkers and Heath, 2005; Kalgutkar et al., 2007; Pelkonen et al., 2008).

CYP inhibition can be categorized as either reversible or irreversible. Irreversible inactivation is generally of greater concern than reversible inhibition as it can result in more profound and prolonged effects (Ghanbari et al., 2006; Kalgutkar et al., 2007). There is increasing awareness that many clinically relevant drug interactions involving CYP inhibition are mediated by irreversible mechanism-based inactivation (MBI) (Ghanbari et al., 2006; Grime et al., 2009). Today potential *in vivo* effects of drug interactions caused by competitive inhibitors can be fairly well predicted from *in vitro* CYP kinetics. The current challenge is to detect time- and concentration-dependent effects of irreversible and quasi-irreversible inactivators among large numbers of early phase compounds in the drug development pipeline (Wienkers and Heath, 2005; Fowler and Zhang, 2008). This is especially important as failure to consider MBI *in vitro* can lead to serious underestimation of drug interaction magnitude *in vivo*, particularly when one is trying to predict drug interactions from *in vitro* data based upon competitive models (Bjornsson et al., 2003; Polasek and Miners, 2007).

DMD Fast Forward. Published on December 9, 2010 as DOI: 10.1124/dmd.110.036376
This article has not been copyedited and formatted. The final version may differ from this version.

The updated regulatory guidances by the U.S. Food and Drug Administration (FDA, 2006) and European Medicines Agency (EMA, 2010) for *in vitro* drug interaction studies include recommendations that drug candidates need to be tested for time-dependent and mechanism-based inactivator properties. Recently, a team of scientists from 16 pharmaceutical research organizations recommended the use of a tiered approach wherein abbreviated assays are first used to determine whether or not new chemical entities demonstrate time-dependent inhibition, followed by more thorough inactivation studies for those that do (Grimm et al., 2009).

Current *in vitro* inactivation research methodologies have been criticized for being significantly influenced by the wide range in experimental conditions, complicating comparison across studies and jeopardizing clinical predictions. In addition, these complex experiments offer limited mechanistic insight (Ghanbari et al., 2006; Riley et al., 2007; Fowler and Zhang, 2008; Obach, 2009; Zhou and Zhou, 2009). Recently, Fairman and co-workers (2007) proposed an alternative *in vitro* approach for the investigation of presteady state kinetics of CYP1A2 inactivation, referred to as progress curve analysis. Progress curve analysis uses an “all-in” approach where the enzyme is exposed simultaneously to probe substrate and inactivator while enzyme activity is monitored throughout the inactivation. This type of analysis has long been an accepted tool for measuring presteady state inhibition kinetics for a variety of physiological enzymes (Fairman et al., 2007; Obach, 2009; Zhou and Zhou, 2009).

Dibenzylfluorescein (DBF) is widely used as a pro-fluorescent probe substrate especially for CYP2C8, CYP2C9, CYP2C19, CYP3A4, and aromatase (CYP19) in high-throughput assays. CYP2C19 was chosen as the target enzyme in this study as it metabolizes several widely used drugs, such as proton pump inhibitors (Pelkonen et al., 2008). Recent data indicate that inhibition

of CYP2C19 may lead to reduction of clinical efficacy of the antithrombotic prodrug clopidogrel (Wallentin, 2009). The DBF assay is based on the general principles originally published by Crespi and co-workers (1997; 2000). The utility of DBF for kinetic assays with continuous data acquisition has been questioned since the initial metabolite of DBF (fluorescein benzyl ester) requires very alkaline conditions for further hydrolysis to maximize the fluorescence intensity (Crespi and Stresser, 2000; Miller et al., 2001).

The purpose of this study was to 1) characterize the properties of DBF as a probe substrate for CYP2C19 enzyme activity and inhibition assays, 2) assess whether DBF can be used as probe substrate in real-time kinetic assay, and 3) demonstrate the use of the progress curve analysis approach for rapid identification of time-dependent CYP inactivators as well as the analysis of key inactivation kinetic parameters.

Materials and Methods

Materials. Isoniazid, trans-2-phenylcyclopropylamine hydrochloride (tranylcypromine), ticlopidine, and fluorescein were purchased from Sigma-Aldrich (St. Louis, MO, USA) and were of the highest purity available. Dibenzylfluorescein (purity >99%) and cDNA-expressed human wild-type CYP2C19 (Supersomes^{TM}) were purchased from BD Biosciences Discovery Labware (Bedford, MA, USA). Fluorescein benzyl ester and fluorescein benzyl ether were synthesized with reagents of commercial high purity quality without further purification unless otherwise mentioned. Reactions were monitored by thin-layer chromatography using aluminum sheets coated with silica gel 60 F245 (0.24 mm) with suitable visualization. The microwave irradiation experiment was carried out in a Biotage Initiator microwave reactor (Biotage, Uppsala, Sweden) in a pressure-rated glass tube. Purifications by flash chromatography were performed on silica gel 60 (0.063- 0.200 mm mesh). ^{1}H and ^{13}C nuclear magnetic resonance (NMR) spectra were recorded on a Bruker Avance AV 500 spectrometer (Bruker Biospin, Fällanden, Switzerland) operating at 500.13 and 125.75 MHz, respectively, using tetramethylsilane (TMS) as an internal standard. The products were also characterized by mass spectrometry with a Finnigan LCQ quadrupole ion trap mass spectrometer (Finnigan MAT, San Jose, CA) equipped with an electrospray ionization source. The purity was determined by elemental analysis (C, H, N) with a ThermoQuest CE Instruments EA 1110-CHNS-O elemental analyzer (CE Instruments, Milan, Italy).

Synthesis of fluorescein benzyl ester (Fig. 1). Fluorescein (800 mg, 2.4 mmol), benzyl alcohol 10 ml and conc. sulphuric acid (1.2 g, 12 mmol) were irradiated with microwaves at 120 ^{o}C for 1 h. The reaction mixture was poured into a water / $NaHCO_3$ (50 ml/ 3 g) solution and treated with

DMD Fast Forward. Published on December 9, 2010 as DOI: 10.1124/dmd.110.036376
This article has not been copyedited and formatted. The final version may differ from this version.

EtOAc. The organic phase was washed with water 3x100 ml and dried with Na_2SO_4 and EtOAc was evaporated in vacuum. The residue was precipitated with Et_2O to remove excess of benzyl alcohol and purified by flash chromatography using petroleum ether/EtOAc as an eluent yielding 50 mg (5 %) of the solid material. ESI-MS: m/z = 423.23 (M+1); ^{1}H NMR δ (ppm) ($CDCl_3$/CD_3OD): 4.93 (s, 2H), 6.62 (d, 2H), 6.65 (d, 2H); 6.90 (dd, 4H), 7.20 (t, 2H), 7.28 (t, 2H), 7.42 (s, 1H), 7.72 (t, 1H), 7.76 (t, 1H), 8.30 (d, 1H). ^{13}C NMR ($CDCl_3$/CD_3OD): 67.58, 103.59, 115.10, 128.11, 128.44, 128.48, 129.85, 130.09, 130.25, 130.30, 131.33, 132.72, 133.96, 134.01, 153.81, 157.16, 165.42. Anal. Calcd for $C_{27}H_{18}O_5$* 0.75 EtOAc: C, 73.76; H, 4.95, Found: C, 74.09; H, 4.66.

Synthesis of fluorescein benzyl ether (Fig. 1). Fluorescein methyl ester (Adamczyk et al., 1999) (1.75 g, 5.05 mmol), benzyl bromide (1.04 g, 6.06 mmol) and potassium carbonate (2.10 g, 15.2 mmol) in DMF (10 ml) were irradiated with microwaves at 75 ^{o}C for 30 min. DMF was evaporated and the residue was purified by the flash chromatography using petroleum ether / EtOAc as an eluent yielding 520 mg (24 %) of the solid material. ^{1}H NMR δ (ppm) ($CDCl_3$): 3.64 (s, 3H), 5.17 (s, 2H), 6.44 (d, 1H), 6.53 (dd, 1H), 6.80 (dd, 1H), 6.84 (d, 1H), 6.89 (d, 1H), 7.03 (d, 1H), 7.31 (d, 1H), 7.41 (m, 5H), 7.66 (t, 1H), 7.73 (t, 1H), 8.24 (d, 1H). The product (140 mg, 0.32 mmol) and lithium iodide (428 mg, 3.21 mmol) were dissolved in pyridine (5 ml) and were irradiated with microwaves at 120 ^{o}C for 1 h. Pyridine was evaporated and the residue was purified by the flash chromatography using petroleum ether / EtOAc as an eluent yielding 60 mg (44 %) of the solid material. ^{1}H NMR δ (ppm) ($CDCl_3$): 5.09 (s, 2H), 6.52 (dd, 1H), 6.63 (d, 1H), 6.67 (s, 1H) 6.68 (s, 1H), 6.71 (d, 1H), 6.84 (t, 1H), 7.16 (d, 1H), 7.39 (m, 5H), 7.61 (t, 1H), 7.66 (t, 1H), 8.01 (d, 1H). ESI-MS: m/z = 421.24 (M-1); ^{13}C NMR ($CDCl_3$): 70.27, 101.85, 103.12, 111.21, 111.28, 112.22, 112.30, 123.98, 125.03, 126.73, 127.47, 128.19, 128.67, 129.09, 129.33,

DMD Fast Forward. Published on December 9, 2010 as DOI: 10.1124/dmd.110.036376
This article has not been copyedited and formatted. The final version may differ from this version.

129.71, 135.09, 136.23, 152.43, 152.48, 153.11, 157.73, 160.47, 169.93. Anal. Calcd for $C_{27}H_{17}O_5Li$*0.1 Hexane: C, 75.86; H, 4.24, Found: C, 75.97; H, 4.59.

CYP-catalyzed metabolism of DBF and effect of base. CYP2C19 catalyzed biotransformation of DBF was analyzed by liquid chromatography-electrospray ionization mass spectrometry (LC-MS). Incubations were conducted in 500-µl volume in Eppendorf tubes using cDNA-expressed recombinant CYP2C19 enzyme. Incubation mixtures for enzyme-catalyzed samples contained 0.1 M Tris-HCl buffer (pH 7.4), 10 µM DBF, 15 pmol CYP2C19 enzyme, and a NADPH-regenerating system (1.13 mM NADP, 12.5 mM isocitric acid, 56.33 mM KCl, 187.5 mM Tris/HCl, pH 7.4, 12.5 mM $MgCl_2$, 0.0125 mM $MnCl_2$, 0.075 U ml^{-1} isocitrate dehydrogenase). Three kinds of blank samples were used: the first did not contain the CYP enzyme, the second lacked the NADPH-regenerating system, and the third lacked DBF. Otherwise the blanks were treated similarly to the enzyme-catalyzed samples. Each sample was assayed in duplicate. The samples were incubated for 45 min at 37°C. The reactions were terminated by rapid cooling to 4°C and after centrifugation, the supernatants were analyzed by LC-MS. Pure DBF, fluorescein benzyl ester, fluorescein benzyl ether, and fluorescein (all 10 µM) were used as standards and were analyzed in the absence and presence of 2 M NaOH. All samples were analyzed with a FinniganLTQ (Thermo, San Jose, CA) mass spectrometer using positive electrospray ionization and full scan or MS/MS measurements. The compounds were separated using a Agilent 1200HPLC system (Waldbronn, Germany) equipped with a 50 x 2 mm Gemini C18 column (Phenomenex, Torrance, CA) with a gradient starting from 10% acetonitrile, 0.1% formic acid and ending with 90% acetonitrile, 0.1% formic acid in 10 min with a flow rate of 200µl/min and injection volume 5 µl. Column temperature was 30°C. The compounds were identified based on their retention times, molecular weights and MS/MS spectra.

DMD Fast Forward. Published on December 9, 2010 as DOI: 10.1124/dmd.110.036376
This article has not been copyedited and formatted. The final version may differ from this version.

Stability of fluorescence intensity. Stability of fluorescence intensity of DBF, fluorescein benzyl ester, fluorescein benzyl ether, and fluorescein (all 1 µM) were characterized at different pH and temperatures (room temperature or 37°C). The buffers were either 100 mM Tris-HCl (pH 7.0 and 7.4) or 100 mM KPO_4 (pH 7.0 and 7.4). All samples were in 150-µl total volume in duplicate in OptiPlate^{TM}-96-well microplates and the fluorescence intensity was measured with a Victor2 plate reader (Perkin-Elmer Life Sciences Wallac, Turku, Finland) in a continuous mode at 1-minute intervals for 90-min at excitation and emission wavelengths of 485 and 535 nm, respectively.

Prerequisites for kinetic assay. The initial prerequisites for a real-time kinetic assay were investigated using the end-point assay procedure by assessing if enzyme activity could be detected without the use of 2 M NaOH. This was carried out by comparing signal-to-noise-ratios between an enzyme-catalyzed sample and two blank (non-enzyme-catalyzed) samples. The experimental conditions were as described in Table 1. The reactions were initiated by adding 50 µl of the NADPH-regenerating system after a 10-min preincubation at 37°C, and were subsequently incubated for 30 min at 37°C in dark. Blank I was similar to the control (enzyme-catalyzed) sample except that 110 µl of 2 M NaOH was added into the wells before addition of the NADPH-regenerating system. Blank II lacked the enzyme. After measuring fluorescence at the end of the 30-min incubation, 110 µl of 2 M NaOH was added into the wells containing control and blank II samples, and the fluorescence was measured again.

Real-time kinetic assay. Real-time kinetic assays were conducted at 37°C in a Victor2 plate scanner using the experimental conditions in Table 1. Blank samples were treated similarly to the enzyme-catalyzed samples but in the absence of CYP enzyme. Reactions were initiated by

DMD Fast Forward. Published on December 9, 2010 as DOI: 10.1124/dmd.110.036376
This article has not been copyedited and formatted. The final version may differ from this version.

addition of DBF (experiment A) or the NADPH-regenerating system (experiment B). Experiment C was conducted by measuring first the substrate in a Victor2 plate scanner for 15-min at 37°C, after which the prewarmed enzyme and the NADPH-regenerating system were added into the wells, and immediately after that the actual reaction incubation and fluorescence data acquisition was carried out at 1-minute intervals for 45 minutes. Each experiment was performed in duplicate. In addition, the linearity of the CYP2C19 catalyzed reaction with respect to enzyme concentration and incubation time was investigated by using varying amounts (0.125–2 pmol) of the enzyme.

Determination of IC_{50}. To compare determination of IC_{50} value between end-point and kinetic assays, IC_{50} value of the known CYP2C19 inhibitor tranylcypromine was assessed using four modified procedures: (A) traditional end-point assay, (B) end-point assay combined with initial measurement of the substrate for 15 min before the reaction initiation, and kinetic assays without (C) and with (D) substrate pre-measurement. The reactions were initiated by adding the enzyme, and were incubated for 30 min at 37°C. In the end-point assays, the reactions were terminated by addition of 110 µl of 2 M NaOH. In the kinetic assays, linear regions of the progress curves were used for the reaction velocity calculations. All IC_{50} values were determined as a mean value from duplicate determinations. Percentages of remaining CYP activity were plotted as a function of logarithm of the molar concentration of tranylcypromine, and the curves were fitted to a sigmoid dose-response equation with Prism 4.0 software (San Diego, CA, USA).

Progress curve analysis. The procedure involving the 15-min initial measurement of substrate as shown in Fig. 3C was used in progress curve analysis. In these experiments, the enzyme is exposed simultaneously to the substrate and inactivator, and enzyme activity is monitored

DMD Fast Forward. Published on December 9, 2010 as DOI: 10.1124/dmd.110.036376
This article has not been copyedited and formatted. The final version may differ from this version.

throughout the process (real-time kinetic assay). Progress curve experiments were carried out by evaluating two known mechanism-based (time-dependent) inactivators, isoniazid and ticlopidine, and one known reversible (time-independent) inhibitor, tranylcypromine. Seven different concentrations of each test compound were used: 2.74–4000 μM for isoniazid, 0.14–100 μM for ticlopidine, and 0.14–100 μM for tranylcypromine. These concentrations were selected to ensure a wide range of inactivation across the 45-min time course. Isoniazid and ticlopidine were dissolved in water, and tranylcypromine was dissolved in acetonitrile (ACN) and then further diluted with water. Consequently, the final solvent concentrations in the incubations did not exceed 2.2 %. Controls were treated similarly but without the presence of inactivators. The obtained fluorescence data were analyzed to determine the key kinetic parameters and mechanistic information of the inactivation process.

Each progress curve were fitted by Eq. 1 (Copeland, 2005) that contains terms for the initial and steady state velocities (v_i and v_S), and for the rate constant for onset of inhibition (k_{obs}), i.e., conversion from the initial velocity phase to the steady state velocity phase.

Equation 1. $$[\text{Product}] = v_s t + \frac{v_i - v_s}{k_{obs}}\left[1 - \exp(-k_{obs} t)\right]$$

K_{obs} values were then plotted against inactivator concentrations, and fitted to Eq. 2 (Fairman et al., 2007):

Equation 2. $$k_{obs} = \frac{k_{inact}[\text{I}]}{K_I(1 + \text{S}/K_m) + [\text{I}]}$$

DMD Fast Forward. Published on December 9, 2010 as DOI: 10.1124/dmd.110.036376
This article has not been copyedited and formatted. The final version may differ from this version.

where k_{inact} is the maximum rate of inactivation, [I] is concentration of inactivator, K_I, is inactivator concentration required for half-maximal inactivation, S is substrate concentration, and K_m is the Henri-Michaelis-Menten constant.

Results

CYP-catalyzed metabolism of DBF and effect of base. The CYP2C19-catalyzed biotransformation of DBF and effect of base were investigated by LC-MS. The retention times, MH^+ ions, and major MS/MS fragment ions for the standards were used for identification of the compounds (Table 2). Fluorescein benzyl ester was formed in the CYP2C19-catalyzed reaction as a major metabolite, and minor amounts of fluorescein benzyl ether were also detected. Fluorescein was not formed at the reaction pH 7.4. In the blank samples, fluorescein benzyl ester, fluorescein benzyl ether, and fluorescein were not formed from DBF. Addition of 2 M NaOH caused decomposition of DBF to fluorescein benzyl ether, and decomposition of fluorescein benzyl ester to fluorescein, whereas fluorescein and fluorescein benzyl ether remained unchanged in the presence of 2 M NaOH. The standard compounds remained unchanged in the absence of 2 M NaOH. The results are presented in Fig. 1.

Stability of fluorescence intensity. The fluorescence intensity of DBF decreased markedly during the first 10 min of the measurement until it reached a steady state (Fig. 2). The fluorescence intensity during the 90-min measurement was the same with the different buffers (Tris-HCl and KPO_4), pH conditions (pH 7.0 and 7.4), and temperatures (room temperature and 37°C). A similar quenching of fluorescence was observed for fluorescein benzyl ester and fluorescein benzyl ether but not for fluorescein (data not shown). At steady state, when compared the amounts of the fluorescence intensity of DBF with the intensities of fluorescein benzyl ether, fluorescein benzyl ester, and fluorescein these were 20-fold, 120-fold and 200-fold higher than that of DBF, respectively.

DMD Fast Forward. Published on December 9, 2010 as DOI: 10.1124/dmd.110.036376
This article has not been copyedited and formatted. The final version may differ from this version.

Prerequisites for kinetic assay. The optimal conditions for the kinetic assay were examined by comparing fluorescence intensities between enzyme-catalyzed sample and two kinds of blank samples, and by evaluating the effects of NaOH on fluorescence intensity. The results are summarized in Table 3. An acceptable signal-to-noise ratio was achieved during the 30-min incubation without addition of 2 M NaOH to the samples, as the fluorescence intensity was 12-fold higher in the enzyme-catalyzed samples than in Blank II (no enzyme) sample. In contrast, the fluorescence intensity was only about 2–3-fold higher in the enzyme-catalyzed samples than in Blank I (NaOH added before initiating the reaction). One important finding was that the signal-to-noise ratio was about 5 times greater between the enzyme sample and blank II than between enzyme sample and blank I. Addition of 2 M NaOH at the end of incubation resulted in only an 1.5-fold increase in fluorescence intensity. The result showed that it is feasible to detect enzyme activity without the use of 2 M NaOH, and blank II is a better choice for assessing background noise compared to blank I.

Real-time kinetic assay. The progress of the CYP-mediated catalytic reaction can be observed from the kinetic readouts as shown in Fig. 3. The fluorescence intensity of DBF is declined to the steady state value during the 15-min initial measurement, allowing for detection of the linear reaction kinetics from the very beginning of the reaction (Fig. 3C).

The time course of CYP2C19-catalyzed reaction with varying amount of the enzyme is presented in Fig. 4. Linear kinetics with respect to enzyme amount and incubation time was evident from the plots. Linear regression analysis of the plot of enzyme amount versus incubation time indicated that the best linearity was obtained with 1–2 pmol of the enzyme.

DMD Fast Forward. Published on December 9, 2010 as DOI: 10.1124/dmd.110.036376
This article has not been copyedited and formatted. The final version may differ from this version.

Determination of IC_{50}. The IC_{50} value of tranylcypromine was determined by the end-point (experiments A and B) and the kinetic assays (experiments C and D). Inhibition of DBF metabolism by tranylcypromine is shown in Fig. 5.

Progress curve analysis. Progress curves for each of the inactivators are shown in Fig. 6. All reaction progress curves without inactivator displayed linear kinetics, and confirmed that the measurements were made during the linear steady state phase of the reaction. For isoniazid and ticlopidine, significant time- and concentration-dependent inactivation of CYP2C19 was observed, and their progress curves were fitted to the Eq. 1 to obtain estimates of k_{obs}, v_i, and v_s at several concentrations. Except for tranylcypromine, best fit lines of the inactivators yielded v_s values of zero (Fig. 6).

The K_{obs} values were replotted against inactivator concentrations, and fitted to the Eq. 2 (Fig. 7). The determined K_I and k_{inact} values are presented in Table 4. Tranylcypromine showed concentration- but not time-dependent inhibition determined by its linear progress curves at each concentration. Thus it was analyzed by linear fitting of each concentration as the relative reaction velocity can be determined from the slope of a linear fit, and IC_{50} value was determined via standard methodologies (4.72 ± 0.30 μM), and then converted to an absolute inhibition constant (K_i 2.36 μM) for substrate affinity and concentration using the Cheng-Prussof equation, where $K_i = IC_{50}/(1 + [S]/K_m)$. All results represent the mean of duplicate determinations.

Discussion

In the present study we describe development of a simple, direct and informative fluorometric method for the assessment of CYP2C19 enzyme inactivation kinetics. The well known inactivators were used to test the method. Isoniazid and ticlopidine were chosen because clinically relevant interactions between them and substrates of CYP2C19 have been reported and they are known to act *via* MBI (Donahue et al., 1997; Tateishi et al., 1999; Nishimura et al., 2003; Richter et al., 2004; Kalgutkar et al., 2007; Venkatakrishnan and Obach, 2007). The selected competitive inhibitor, tranylcypromine, is commonly used as positive control compound for CYPC19 inhibition studies (BD Gentest, 2000; Lin et al., 2007).

The data show that 2 M NaOH is not required for the enzyme activity determinations using DBF as the probe substrate as the fluorescence intensity of the metabolite formed (fluorescein benzyl ester) is 120-fold higher than that of DBF. The transformation of fluorescein benzyl ester to fluorescein in the presence of 2 M NaOH is consistent with the reports of its use in the end-point assays (Miller et al., 2001; Hong et al., 2008). However, it is not desirable that at the same time DBF is transformed to fluorescein benzyl ether in the presence of 2 M NaOH which also increases the background fluorescence intensity and causes significant deterioration in the sensitivity, i.e., signal-to-noise-ratio.

Therefore, CYP2C19 enzyme activity can be followed in real time using DBF as the substrate. The product formation is linear from the very beginning of the reaction, and the IC_{50} values calculated from the progress curves are comparable with the results obtained with the traditional end-point assay and correlated well with literature data (a range of 1.9–9 μM) (BD Gentest, 2000;

DMD Fast Forward. Published on December 9, 2010 as DOI: 10.1124/dmd.110.036376
This article has not been copyedited and formatted. The final version may differ from this version.

Dierks et al., 2001; Lin et al., 2007). Kinetic assay provides the most reliable means of accurately determining reaction velocity from the slope of a plot of signal versus time, i.e., it is purely a result from the enzyme activity itself. Based on these experiments, the observed spontaneous quenching of DBF fluorescence is due to some fluorometric phenomenon instead of decomposition of the compound. The other related compounds possess higher fluorescence intensities than DBF.

The full progress curve of an enzymatic reaction contains an abundance of valuable kinetic information, and allows investigation of both reversible and irreversible components of the reaction mechanisms, and thus provides more information in one experiment. All irreversible enzyme inactivators display slow binding kinetics in progress curve analysis, and the slow onset of inhibition is best studied by following progress curves. Time-dependent inactivation converts the linear progress curve seen in the absence of the inactivator into a curvilinear function so that the degree of inhibition at a fixed concentration of compound will vary over time. Thus the enzyme reaction progress curve will be nonlinear, and reflect two distinct velocities for the reaction (Copeland, 2005). This behavior was seen with the known time-dependent inactivators isoniazid and ticlopidine but not with the known time-independent inhibitor, tranylcypromine.

For time-dependent irreversible/quasi-irreversible inactivators, the value of k_{obs} is generally expected to increase over a certain range of inactivator concentrations and then to undergo saturation at higher concentrations (Kalgutkar et al., 2007). The first step involves reversible binding of the inactivator to the enzyme, often under rapid equilibrium conditions. For mechanism-based inactivators, the second step involves some bioactivation/chemistry of the covalent bond formation or transformation into metabolic intermediate (MI) products that

DMD Fast Forward. Published on December 9, 2010 as DOI: 10.1124/dmd.110.036376
This article has not been copyedited and formatted. The final version may differ from this version.

coordinate tightly to the heme iron atom of CYP enzyme. This behavior (saturation) was also seen with isoniazid and ticlopidine in this study pointing to a two-step inactivation mechanism.

All mechanism-based inactivators are competitive with the normal substrate of the enzyme, because they rely on the catalytic mechanism of the enzyme active site. The presence of substrate can hinder the access of the inactivator to the enzyme, i.e. the substrate has to be at a relatively low concentration (K_m) so that it does not completely block the enzyme inactivation process (Ghanbari et al., 2006). For that reason, the probe substrate at the concentration corresponding to its measured apparent K_m (data not shown) was used in the experiments and this was taken into account when determining kinetic constants of the inactivation. The determined inactivation kinetic constants (K_I and k_{inact}) for isoniazid and ticlopidine correlated with published data (Wen et al., 2002; Nishimura et al., 2003; Polasek et al., 2006; Kalgutkar et al., 2007; Venkatakrishnan and Obach, 2007; Nishiya et al., 2009).

This progress curve analysis methodology allows also estimates of the initial binding equilibrium as reflected in the magnitude of reduction of v_i by the inactivator against respective control, as described by Fairman and co-workers (Fairman et al., 2007). In our study, v_i was plotted against initial inactivator concentration but they showed no significant inhibition across the concentration range (<40–50 % inhibition at any concentration tested) so that no estimation of K_i could be made.

In conclusion, time-dependent inhibition is one of the major distinguishing features between reversible and irreversible/quasi-irreversible inhibition. It thus provides a useful screening approach for identifying potential mechanism-based inactivators in early drug interaction studies

for pharmaceuticals under development. This is especially important, because it has become widely appreciated that detection and amelioration of time-dependent inactivation is a crucial aspect in drug interaction optimization for novel compounds (Polasek and Miners, 2007; Fowler and Zhang, 2008). DBF characterization, kinetic assay, and the progress curve analysis approach together offer a new response and improvement for the current challenge. The present work has shown that the widely used CYP substrate, DBF, is suitable for use in a progress curve analysis approach, i.e. this is a rapid and reliable method that can be used as an initial screen to help identify compounds that require more detailed investigations. However, this approach will require further evaluation with a broader set of CYP enzymes and inactivators before it is fully exploitable.

DMD Fast Forward. Published on December 9, 2010 as DOI: 10.1124/dmd.110.036376
This article has not been copyedited and formatted. The final version may differ from this version.

Acknowledgements

We thank Ms Hannele Jaatinen for technical help and Dr Ewen MacDonald for contribution to the preparation of the manuscript. The research was financially supported by the Finnish Graduate School of Toxicology.

Authorship Contributions

Participated in research design: Salminen, Venäläinen, and Raunio.

Conducted experiments: Salminen, and Auriola.

Contributed new reagents or analytic tools: Leppänen.

Performed data analysis: Salminen.

Wrote or contributed to the writing of the manuscript: Salminen, Venäläinen, Pasanen, Auriola, Juvonen, and Raunio.

References

Adamczyk M, Grote J and Moore JA (1999) Chemoenzymatic synthesis of 3'-O-(carboxyalkyl)fluorescein labels. *Bioconjug Chem* **10**:544-547.

BD Gentest (2000) A high throughput method for measuring cytochrome P450 inhibition. Available at: http://www2.bdbiosciences.com/discovery_labware/gentest/products/HTS_KITS/HTS/hts_summary.shtml

Bjornsson TD, Callaghan JT, Einolf HJ, Fischer V, Gan L, Grimm S, Kao J, King SP, Miwa G, Ni L, Kumar G, McLeod J, Obach SR, Roberts S, Roe A, Shah A, Snikeris F, Sullivan JT, Tweedie D, Vega JM, Walsh J and Wrighton SA (2003) The conduct of in vitro and in vivo drug-drug interaction studies: A PhRMA perspective. *J Clin Pharmacol* **43**:443-469.

Copeland RA (2005) *Evaluation of enzyme inhibitors in drug discovery. A guide for medicinal chemists and pharmacologists.* John Wiley & Sons, Inc., Hoboken, New Jersey.

Crespi CL, Miller VP and Penman BW (1997) Microtiter plate assays for inhibition of human, drug-metabolizing cytochromes P450. *Anal Biochem* **248**:188-190.

Crespi CL and Stresser DM (2000) Fluorometric screening for metabolism-based drug-drug interactions. *J Pharmacol Toxicol □ethods* **44**:325-331.

Dierks EA, Stams KR, Lim HK, Cornelius G, Zhang HL and Ball SE (2001) A method for the simultaneous evaluation of the activities of seven major human drug-metabolizing cytochrome P450s using an in vitro cocktail of probe substrates and fast gradient liquid chromatography tandem mass spectrometry. *Drug Metab Dispos* **29**:23-29.

Donahue SR, Flockhart DA, Abernethy DR and Ko JW (1997) Ticlopidine inhibition of phenytoin metabolism mediated by potent inhibition of CYP2C19. *Clin Pharmacol Ther* **62**:572-577.

EMA (2010) Guideline on the investigation of drug Interactions. EMEA/CHMP/EWP/125211/10. Available at: http://www.emea.europa.eu/htms/human/humanguidelines/efficacy.htm

Fairman DA, Collins C and Chapple S (2007) Progress curve analysis of CYP1A2 inhibition: A more informative approach to the assessment of mechanism-based inactivation? *Drug Metab Dispos* **35**:2159-2165.

FDA (2006) Guidance for industry. Drug interaction studies - study design, data analysis, and implications for dosing and labeling. Available at: http://www.fda.gov/downloads/Drugs/GuidanceComplianceRegulatoryInformation/Guidances/ucm072101.pdf

Fowler S and Zhang HJ (2008) In vitro evaluation of reversible and irreversible cytochrome P450 inhibition: Current status on methodologies and their utility for predicting drug-drug interactions. *Aaps Journal* **10**:410-424.

Ghanbari F, Rowland-Yeo K, Bloomer JC, Clarke SE, Lennard MS, Tucker GT and Rostami-Hodjegan A (2006) A critical evaluation of the experimental design of studies of mechanism based enzyme inhibition, with implications for in vitro-in vivo extrapolation. *Curr Drug Metab* **7**:315-334.

Grime KH, Bird J, Ferguson D and Riley RJ (2009) Mechanism-based inhibition of cytochrome P450 enzymes: An evaluation of early decision making in vitro approaches and drug-drug interaction prediction methods. *Eur J Pharm Sci* **36**:175-191.

Grimm SW, Einolf HJ, Hall SD, He K, Lim HK, Ling KHJ, Lu C, Nomeir AA, Seibert E, Skordos KW, Tonn GR, Van Horn R, Wang RW, Wong YN, Yang TJ and Obach RS (2009) The Conduct of in Vitro Studies to Address Time-Dependent Inhibition of Drug-Metabolizing Enzymes: A Perspective of the Pharmaceutical Research and Manufacturers of America. *Drug Metab Dispos* **37**:1355-1370.

Hong Y, Cho M, Yuan YC and Chen S (2008) Molecular basis for the interaction of four different classes of substrates and inhibitors with human aromatase. *Biochem Pharmacol* **75**:1161-1169.

Kalgutkar AS, Obach RS and Maurer TS (2007) Mechanism-based inactivation of cytochrome P450 enzymes: Chemical mechanisms, structure-activity relationships and relationship to clinical drug-drug interactions and idiosyncratic adverse drug reactions. *Curr Drug Metab* **8**:407-447.

Lin T, Pan K, Mordenti J and Pan L (2007) In vitro assessment of cytochrome P450 inhibition: strategies for increasing LC/MS-based assay throughput using a one-point IC(50) method and multiplexing high-performance liquid chromatography. *J Pharm Sci* **96**:2485-2493.

Miller VP, Stresser D, Crespi CL and Charles L (2001) The use of fluorescein aryl ethers in high throughput cytochrome P450 inhibition assays. PCT Int. Appl. Patent No. WO 2001014361 A1

Nishimura Y, Kurata N, Iwase M and Yasuhara H (2003) Mechanism-based inactivation of human CYP1A2 and CYP2C19 mediated metabolism by isoniazid. *Drug Metab Rev* **35**:100.

Nishiya Y, Hagihara K, Kurihara A, Okudaira N, Farid NA, Okazaki O and Ikeda T (2009) Comparison of mechanism-based inhibition of human cytochrome P450 2C19 by ticlopidine, clopidogrel, and prasugrel. *Xenobiotica* **39**:836-843.

Obach RS (2009) Predicting drug-drug interactions from in vitro drug metabolism data: challenges and recent advances. *Current Opinion in Drug Discovery & Development* **12**:81-89.

Pelkonen O, Turpeinen M, Hakkola J, Honkakoski P, Hukkanen J and Raunio H (2008) Inhibition and induction of human cytochrome P450 enzymes: current status. *Arch Toxicol* **82**:667-715.

Polasek TM, Elliot DJ, Somogyi AA, Gillam EM, Lewis BC and Miners JO (2006) An evaluation of potential mechanism-based inactivation of human drug metabolizing cytochromes P450 by monoamine oxidase inhibitors, including isoniazid. *Br J Clin Pharmacol* **61**:570-584.

Polasek TM and Miners JO (2007) In vitro approaches to investigate mechanism-based inactivation of CYP enzymes. *Expert Opin Drug Metab Toxicol* **3**:321-329.

Richter T, Murdter TE, Heinkele G, Pleiss J, Tatzel S, Schwab M, Eichelbaum M and Zanger UM (2004) Potent mechanism-based inhibition of human CYP2B6 by clopidogrel and ticlopidine. *J Pharmacol Exp Ther* **308**:189-197.

Riley RJ, Grime K and Weaver R (2007) Time-dependent CYP inhibition. *Expert Opin Drug Metab Toxicol* **3**:51-66.

Tateishi T, Kumai T, Watanabe M, Nakura H, Tanaka M and Kobayashi S (1999) Ticlopidine decreases the in vivo activity of CYP2C19 as measured by omeprazole metabolism. *Br J Clin Pharmacol* **47**:454-457.

Wallentin L (2009) P2Y(12) inhibitors: differences in properties and mechanisms of action and potential consequences for clinical use. *Eur Heart J* **30**:1964-1977.

Wen X, Wang JS, Neuvonen PJ and Backman JT (2002) Isoniazid is a mechanism-based inhibitor of cytochrome P450 1A2, 2A6, 2C19 and 3A4 isoforms in human liver microsomes. *Eur J Clin Pharmacol* **57**:799-804.

Venkatakrishnan K and Obach RS (2007) Drug-drug interactions via mechanism-based cytochrome P450 inactivation: Points to consider for risk assessment from in vitro data and clinical pharmacologic evaluation. *Curr Drug Metab* **8**:449-462.

Wienkers LC and Heath TG (2005) Predicting in vivo drug interactions from in vitro drug discovery data. *Nat Rev Drug Discov* **4**:825-833.

Zhou ZW and Zhou SF (2009) Application of mechanism-based CYP inhibition for predicting drug-drug interactions. *Expert Opin Drug Metab Toxicol* **5**:579-605.

Legends for figures

Figure 1. Structures of a probe substrate dibenzylfluorescein (DBF), and fluorescent products. DBF is dealkylated by CYP to form a fluorescein benzyl ester which is further hydrolyzed to fluorescein by NaOH (if present). Addition of 2 M NaOH causes also decomposition of DBF to fluorescein benzyl ether.

Figure 2. Fluorescence intensity of 1 μM dibenzylfluorescein (DBF) as a function of time in different conditions.

Figure 3. Representative progress curves for CYP2C19 enzyme activity: (A) reaction initiated by adding substrate [r^2 value of the linear regression of the enzyme-catalyzed (control) reaction curve 0.987]; (B) reaction initiated by adding the NADPH-regenerating system (r^2 = 0.997); and (C) reaction initiated after 15-min pre-measurement of the substrate by adding the NADPH-regenerating system and the enzyme (r^2 = 0.997).

Figure 4. (A) Progress curves of CYP2C19-mediated fluorescence formation with different amounts of the enzyme. (B) The slopes of the lines from (A) plotted as a function of enzyme amount (pmol).

Figure 5. IC_{50} values of tranylcypromine with end-point (A and B) and kinetic (C and D) assays excluding (A and C) and including (B and D) 15-min initial measurement of substrate.

Figure 6. Representative progress curves of CYP2C19 inactivation. Tranylcypromine (A) reveals no time-dependent inhibition as the curves indicate linear best fits. The known mechanism-based inactivators, isoniazid (B) and ticlopidine (C), exhibit time-dependent inactivation.

Figure 7. Plots of k_{obs} against inactivator concentration for isoniazid (A) and ticlopidine (B) indicate a two-step inactivation mechanism due to a saturable step before inactivation.

DMD Fast Forward. Published on December 9, 2010 as DOI: 10.1124/dmd.110.036376
This article has not been copyedited and formatted. The final version may differ from this version.

Table 1. Experimental conditions in CYP2C19 enzyme activity and inhibition assays in a 150-µl incubation volume.

Tris-HCl, pH 7.4	100 mM
Substrate (DBF) concentration	1.0 µM (equals K_m)
Enzyme (human recombinant CYP2C19)	1.5 pmol
NADPH-regenerating system	50 µl
Incubation time at 37°C	30–60 min
Excitation / Emission wavelengths (nm)	485 / 535

Table 2. LC/MS characteristics of DBF, fluorescein, fluorescein benzyl ester, and fluorescein benzyl ether.

Compound	Retention time	M^+H^+	MS/MS fragment ions
dibenzylfluorescein	9.84	*m/z* 513.4	*m/z* 485, 421, 345, 333
fluorescein	7.25	*m/z* 333.2	*m/z* 305, 287 271
fluorescein benzyl ester	7.28	*m/z* 423.3	*m/z* 361, 345, 317
fluorescein benzyl ether	9.75	*m/z* 423.3	*m/z* 395, 377, 345

DMD Fast Forward. Published on December 9, 2010 as DOI: 10.1124/dmd.110.036376
This article has not been copyedited and formatted. The final version may differ from this version.

Table 3. The signal-to-noise-ratios of enzyme-catalyzed reactions.

Blank	Measurement	
	Immediately after incubation	After the 1st measurement, 2 M NaOH was added into the wells which did not contain it
	Fold difference between enzyme-catalyzed and blank samples	
[a]Blank I	2.4	3.5
[b]Blank II	11.9	17.9

[a]As enzyme-catalyzed sample but 2M NaOH added into samples before initiating the reactions;

[b]As enzyme-catalyzed sample but in the absence of enzyme.

DMD Fast Forward. Published on December 9, 2010 as DOI: 10.1124/dmd.110.036376
This article has not been copyedited and formatted. The final version may differ from this version.

Table 4. Inactivation kinetic constants for isoniazid and ticlopidine.

Inactivator	Determined		Published Data		References
	K_I (μM)	k_{inact} (min^{-1})	K_I (μM)	k_{inact} (min^{-1})	
Isoniazid	250.5 ± 34	0.137 ± 0.006	112	0.090	(Wen et al., 2002)
			255	0.020	(Nishimura et al., 2003)
			79.3	0.039	(Polasek et al., 2006)
Ticlopidine	1.96 ± 0.5	0.135 ± 0.009	1.65	0.192	(Venkatakrishnan and Obach, 2007)
			4.30	0.097	(Kalgutkar et al., 2007)
			3.32	0.074	(Nishiya et al., 2009)

Figure 1.

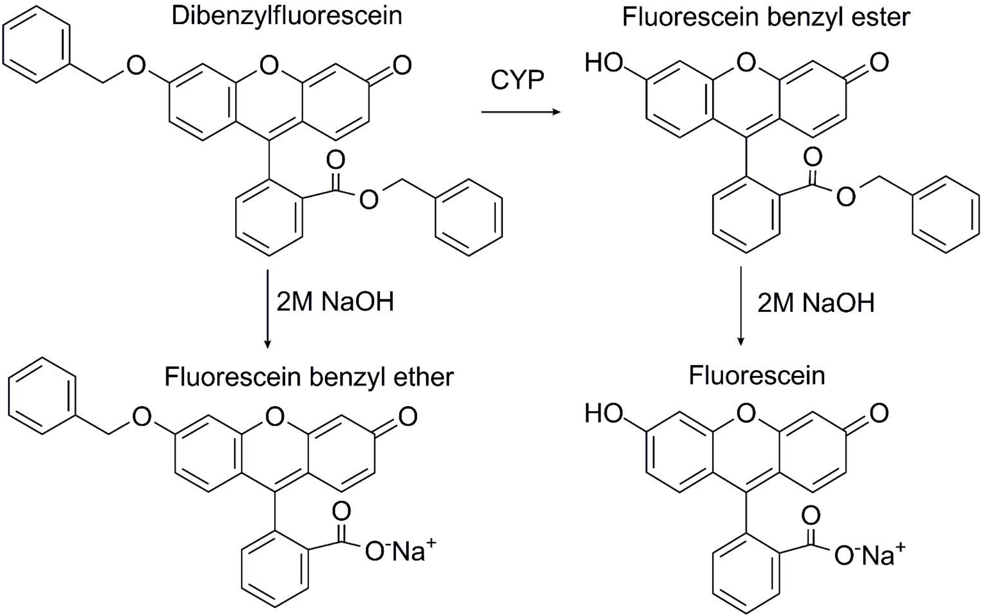
Dibenzylfluorescein
CYP
Fluorescein benzyl ester
2M NaOH
2M NaOH
Fluorescein benzyl ether
Fluorescein

Figure 2.

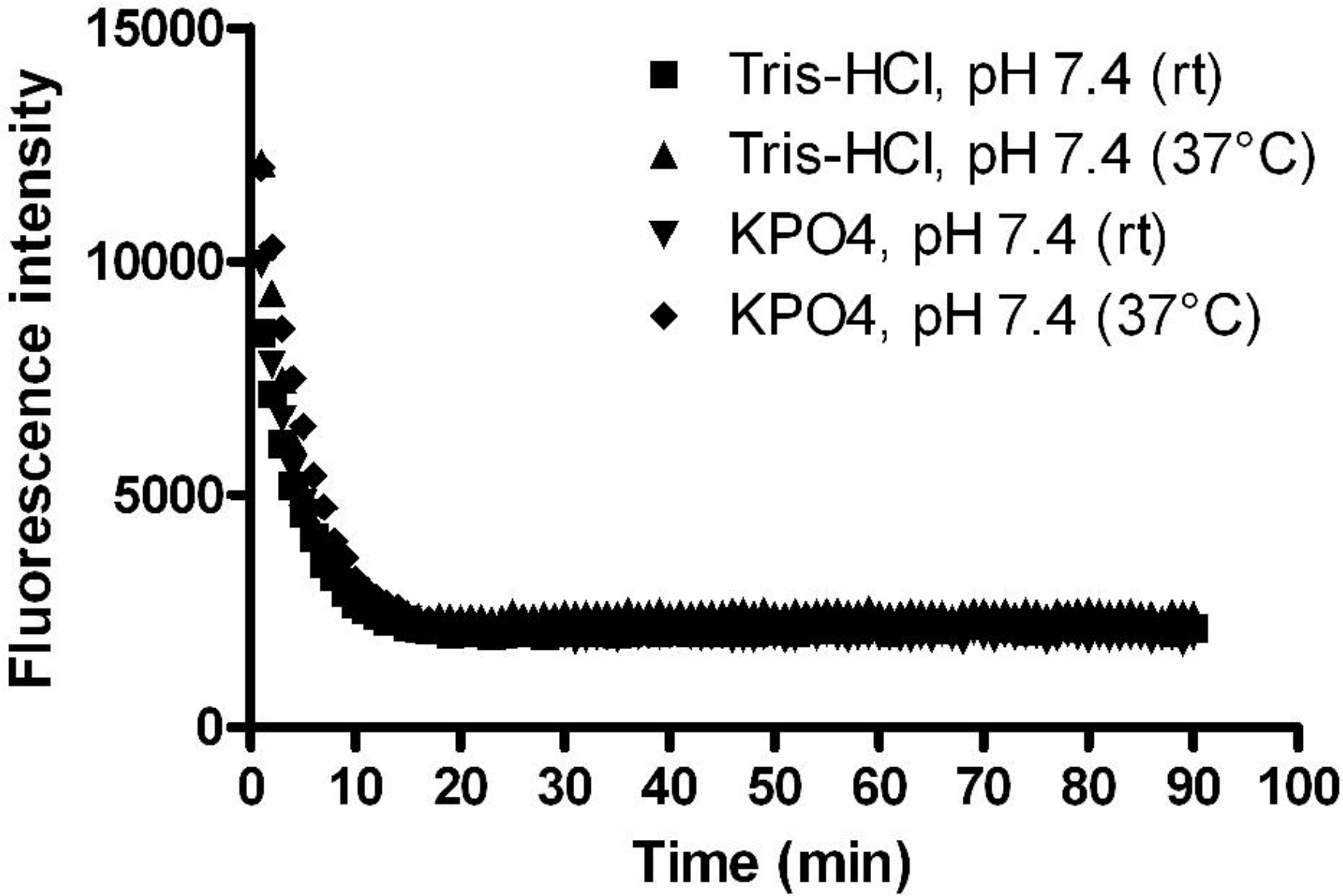
15000
10000
5000
0
Fluorescence intensity
0
10
20
30
40
50
60
70
80
90
100
Time (min)
Tris-HCl, pH 7.4 (rt)
Tris-HCl, pH 7.4 (37°C)
KPO4, pH 7.4 (rt)
KPO4, pH 7.4 (37°C)

Figure 3.

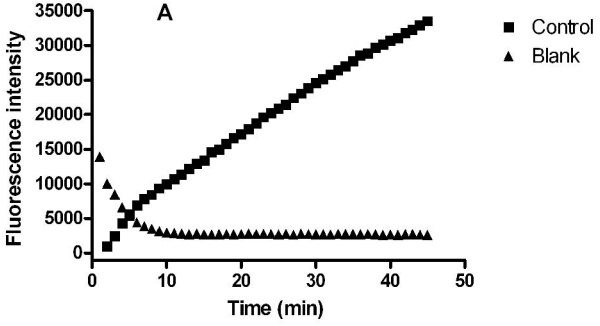
A
Fluorescence intensity
35000
30000
25000
20000
15000
10000
5000
0
0
10
20
30
40
50
Time (min)
Control
Blank

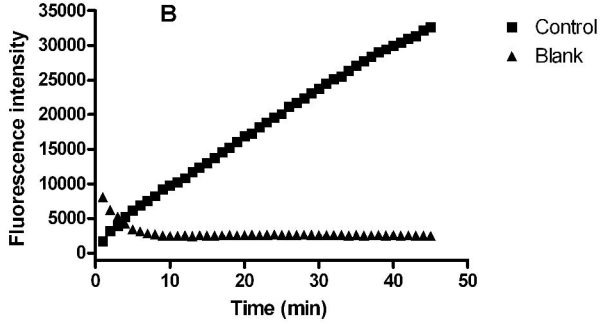
B
Fluorescence intensity
35000
30000
25000
20000
15000
10000
5000
0
0
10
20
30
40
50
Time (min)
Control
Blank

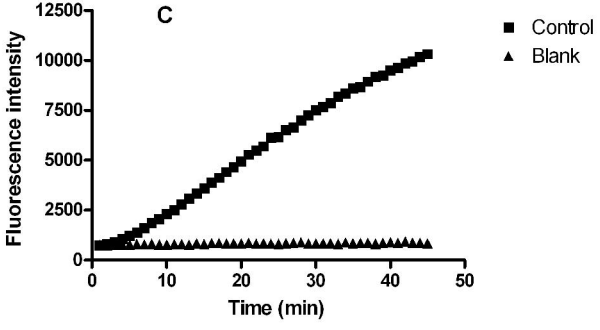
C
Fluorescence intensity
12500
10000
7500
5000
2500
0
0
10
20
30
40
50
Time (min)
Control
Blank

Figure 4.

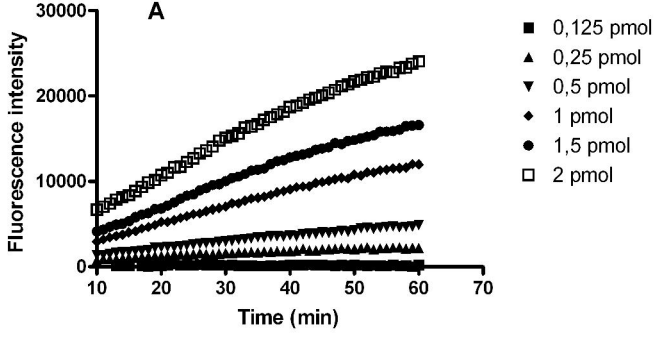
A
Fluorescence intensity
30000
20000
10000
0
10
20
30
40
50
60
70
Time (min)
0,125 pmol
0,25 pmol
0,5 pmol
1 pmol
1,5 pmol
2 pmol

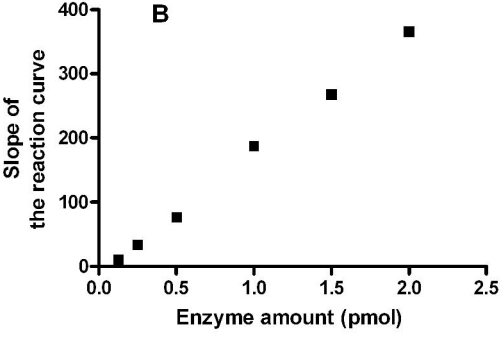
B
Slope of the reaction curve
400
300
200
100
0
0.0
0.5
1.0
1.5
2.0
2.5
Enzyme amount (pmol)

Figure 5.

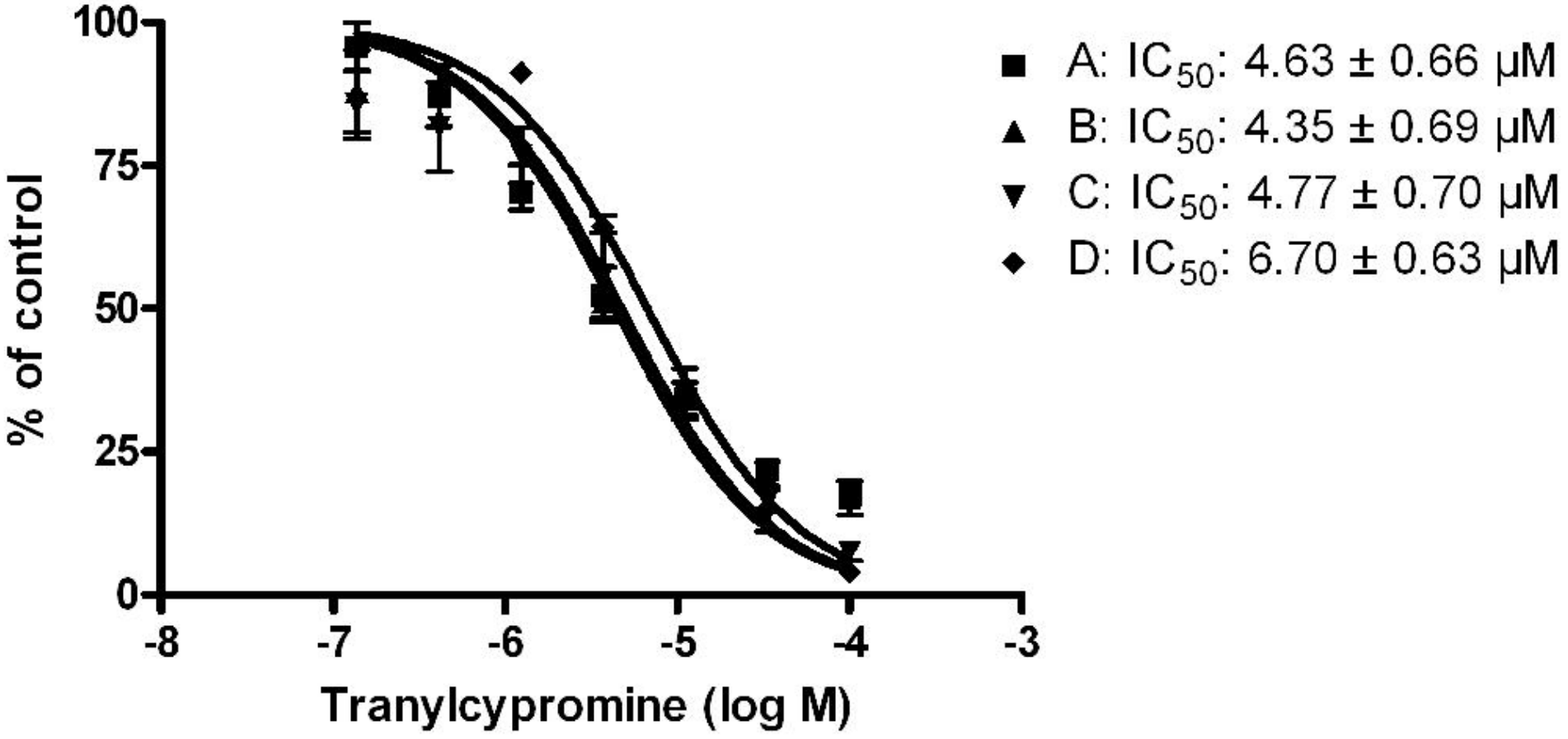
100
75
50
25
0
% of control
-8
-7
-6
-5
-4
-3
Tranylcypromine (log M)
A: IC50: 4.63 ± 0.66 µM
B: IC50: 4.35 ± 0.69 µM
C: IC50: 4.77 ± 0.70 µM
D: IC50: 6.70 ± 0.63 µM

Figure 6.

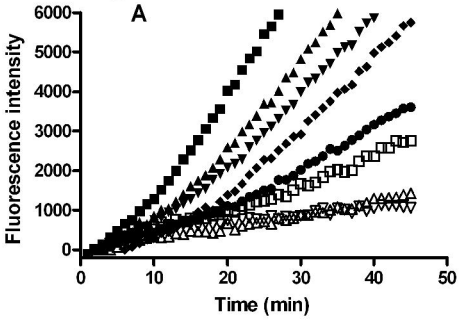
A
Fluorescence intensity
Time (min)
0
1000
2000
3000
4000
5000
6000
0
10
20
30
40
50


Control
1,563 µM
3,125 µM
6,25 µM
12,5 µM
25 µM
50 µM
100 µM

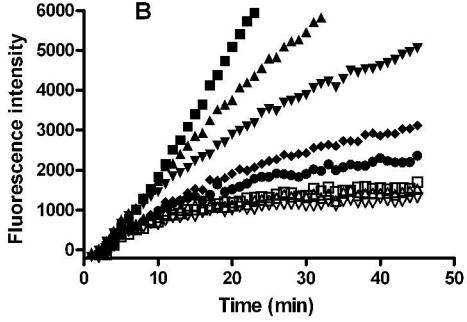
B
Fluorescence intensity
Time (min)
0
1000
2000
3000
4000
5000
6000
0
10
20
30
40
50

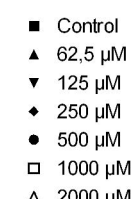
Control
62,5 µM
125 µM
250 µM
500 µM
1000 µM
2000 µM
4000 µM

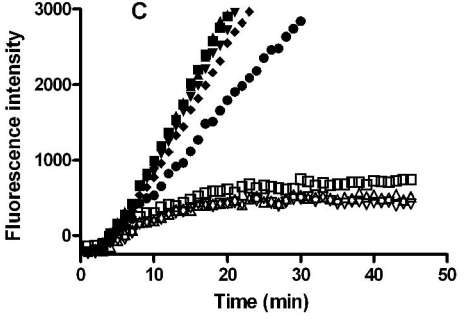
C
Fluorescence intensity
Time (min)
0
1000
2000
3000
0
10
20
30
40
50


Control
0,137 µM
0,412 µM
1,23 µM
3,70 µM
11,1 µM
33,3 µM
100 µM

Figure 7.

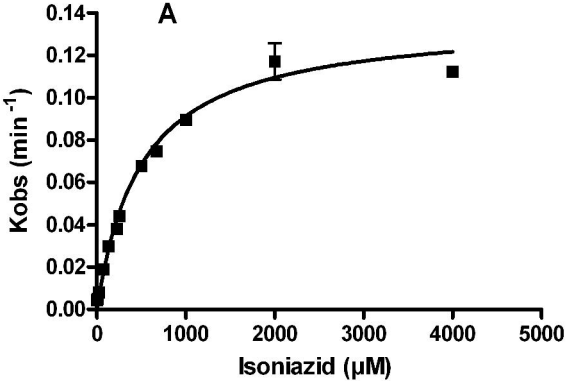
A
Kobs (min-1)
0.14
0.12
0.10
0.08
0.06
0.04
0.02
0.00
0
1000
2000
3000
4000
5000
Isoniazid (μM)

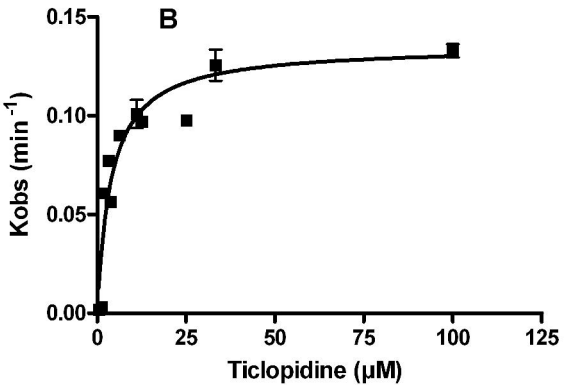
B
Kobs (min-1)
0.15
0.10
0.05
0.00
0
25
50
75
100
125
Ticlopidine (μM)